BRAIN CONNECTIVITY
Volume 8, Number 3, 2018

DOI: 10.1089/brain.2017.0517

The Not-So-Global Blood Oxygen Level-Dependent Signal

Jacob Billings[1] and Shella Keilholz[1,2]

Abstract

Global signal regression is a controversial processing step for resting-state functional magnetic resonance imaging, partly because the source of the global blood oxygen level-dependent (BOLD) signal remains unclear. On the one hand, nuisance factors such as motion can readily introduce coherent BOLD changes across the whole brain. On the other hand, the global signal has been linked to neural activity and vigilance levels, suggesting that it contains important neurophysiological information and should not be discarded. Any widespread pattern of coordinated activity is likely to contribute appreciably to the global signal. Such patterns may include large-scale quasiperiodic spatiotemporal patterns, known also to be tied to performance on vigilance tasks. This uncertainty surrounding the separability of the global BOLD signal from concurrent neurological processes motivated an examination of the global BOLD signal's spatial distribution. The results clarify that although the global signal collects information from all tissue classes, a diverse subset of the BOLD signal's independent components contribute the most to the global signal. Further, the timing of each network's contribution to the global signal is not consistent across volunteers, confirming the independence of a constituent process that comprises the global signal.

Keywords: blood oxygen level-dependent (BOLD) signal; global BOLD signal; global signal regression; noise; quasi-periodic patterns (QPPs); resting-state functional magnetic resonance imaging (rs-fMRI)

Introduction

The global blood oxygen level-dependent (BOLD) signal, obtained by averaging the signal from all voxels across each time point of a resting-state functional magnetic resonance imaging (rs-fMRI) scan, has had a contentious decade. The vector was originally proposed as a regression term to minimize contributions from noise in functional connectivity experiments. Motivated by this rationale, a series of studies demonstrated the use of global signal regression (GSR) to increase inter-network contrast (Fox et al., 2009; Murphy et al., 2009). An effect of GSR is that some correlations within the brain are driven negative, creating problems in interpreting GSR-denoised functional connectivity data.

Clearly, there are arguments to be made both for and against GSR (see Murphy et al., 2013 for an excellent review). The use of GSR promotes spatial specificity in functional networks (Fox et al., 2009). Shirer et al. found that regression of global signal reduced noise but at the expense of test-retest reliability (Shirer et al., 2015). In animal models, GSR has been used to control for different levels of baseline blood flow and metabolism in the brain due to varying levels of isoflurane anesthesia (Liu et al., 2013). A positron emission tomography and rs-fMRI study in humans showed a similar effect, with the global signal amplitude linked to changes in fludeoxyglucose metabolism (Thompson et al., 2016). In one study that compared simultaneously recorded bandlimited power and BOLD correlation from two sites in the brain, GSR improved the fidelity of the BOLD signal to changes in simultaneously recorded local field potentials (Thompson et al., 2013b). These studies suggest that if the global signal has a neural origin, it is unlikely to lie in the coordinated, time-varying modulations of neural activity that would ideally be detected with resting-state magnetic resonance imaging (MRI) and that its removal may improve sensitivity to the signal of interest.

On the other hand, the global BOLD signal amplitude is negatively correlated to electroencephalography (EEG) measures of vigilance in subjects with their eyes closed (Wong et al., 2013), suggesting that it might contain information about important neurophysiological processes that should not be discarded. Neural activity from a single electrode is correlated with the cerebral blood volume-weighted signal from much of the brain, although at variable time delays

[1]Program in Neuroscience, Graduate Division of Biological and Biomedical Sciences, Emory University, Atlanta, Georgia.
[2]Department of Biomedical Engineering, Emory/Georgia Institute of Technology, Atlanta, Georgia.

(Scholvinck et al., 2010). Changes in broadband EEG power are associated with changes in global signal at delays approximating the hemodynamic delay (Wen and Liu, 2016). Others have even shown that global activation can be detected in fMRI provided enough averages are acquired (Gonzalez-Castillo et al., 2012). These findings all suggest that the global signal is more than a nuisance. Further, GSR can distort differences between groups (Saad et al., 2012). The global signal itself can distinguish patient groups from healthy controls (Hahamy et al., 2014; Yang et al., 2014), though some of these differences may arise from changes in head motion or in vascular tone.

A brief perusal of these findings raises the question of exactly what constitutes the global BOLD signal. Because it is calculated as the sum of signals from all brain voxels, patterns of widespread activation might provide substantial contributions to the global signal. For example, the application of a recursive pattern-finding algorithm to resting-state BOLD activity has identified quasi-periodic patterns (QPPs) that exhibit a large-scale spatial structure involving periodic activation and deactivation of two brain networks—the default-mode network (DMN) and the task-positive network (TPN) (Majeed et al., 2011; Thompson et al., 2014b). Using a recursive algorithm, Majeed et al. (2011) averaged spatiotemporal chunks of a resting-state BOLD scan that most strongly correlated with a randomly seeded spatiotemporal chunk. Calculation of a dominant QPP template enabled the observation of propagating BOLD activation along the cortex, over time, within individual and group-level scans (Majeed et al., 2009, 2011). QPPs are linked to infraslow activity (Thompson et al., 2014b; Pan et al., 2013) and appear to be separable from the aperiodic changes that are expected to be more cognitively relevant (Thompson et al., 2014a; Thompson et al., 2015). Both infraslow (0.01–0.1 Hz) electrical activity and TPN/DMN activity have been linked to performance, particularly on tasks with a strong attentional component (Fox et al., 2007; Kelly et al., 2008; Monto et al., 2008; Thompson et al., 2013a). Moreover, recent work shows that the phase of the QPP predicts reaction time on a simple vigilance task (Abbas et al., 2016). A growing body of work links the global signal to vigilance as well (Wong et al., 2013, 2016).

The similarities between QPPs and the global signal motivated a more thorough examination of the characteristics of the global BOLD signal to determine whether QPPs are a substantial contributor. To this end, we examined the spatial distribution of the global BOLD signal from several directions: across brain tissue classes, across individuals, across functional brain networks, across spectra, and through time. The findings suggest that the global BOLD signal is not so global after all. Rather, it is a weighted sum of nonstationary and independent BOLD activations.

Methods

Data acquisition

Neuroimaging data were downloaded through the 1000 Functional Connectomes Project.* The data were acquired as part of the *Enhanced Rockland Sample Multiband Imaging Test-Retest Pilot Dataset*, uploaded by the Nathan Kline Institute for Psychiatric Research† (Nooner et al., 2012). A total of 31 volunteer datasets of 32 total datasets were used for this study. One dataset was excluded after becoming corrupted during automated co-registration. Volunteers were 44 ± 18 years old, with 21 women and 10 men. Thirty volunteers were right-handed; one had no preference.

Whole brain images were acquired on a 3T Siemens Magnetome TriTom (multiband echo planar imaging [EPI]; repetition time [TR] 645 msec; echo time [TE] 30 msec; 40 slices; field of view [FOV] 22.2×22.2 cm; 3 mm isotropic voxels; 900 images). A 32-channel anterior/posterior head coil facilitated multiband EPI imaging at high temporal resolution. An MPRAGE scan was acquired to facilitate alignment (TR 1900 msec; TE 2.52 msec; 176 slices; FOV 25×25 cm; 1 mm isotropic voxels).

Preprocessing

A series of preprocessing steps were carried out over the entire dataset to bring data points into temporal and spatial alignment. These steps were conducted by using revision 6470 of the Statistical Parametric Mapping MATLAB toolbox.‡ Slice timing mismatches were corrected per each slice's multiband acquisition time. Within-scan images were realigned to correct for movement between repetitions. Each scan's mean realigned image was co-registered to the volunteer's structural image. Structural images were segmented into five tissue classes: gray matter, white matter, cerebrospinal fluid (CSF), bone, and soft tissue. A warping matrix was evaluated and used to normalize each scan from subject space to Montreal Neurological Institute (MNI) space. Images were smoothed by an $8 \times 8 \times 8$ mm Gaussian kernel. Finally, volunteer images were realigned to the group mean of the functional images.

To facilitate correlation-based comparison of spontaneous BOLD variability, we identically distributed voxel time series to zero mean and unit variance (Biswal et al., 1995; Buzsáki and Draguhn, 2004; Majeed et al., 2011). As movement artifacts may instantiate inter-regional correlations in the BOLD signal, voxel-wise signals were linearly regressed against three translational movement terms, three rotational movement terms, and their squares. Motion terms were declared as deviations from each volunteer's central orientation during the scan.

Data analysis

After preprocessing, a global signal was calculated for each scan as the mean signal from all image voxels. The Pearson correlation between the global signal and each voxel's signal defines the voxel-wise Global Signal Correlation. The cross-correlation between voxel-wise and the global signal was also assessed to help observe any periodic trends. Cross-correlation amplitudes were normalized to unit autocorrelation at time-lag zero.

Because the brain is internally organized into networks spanning multiple voxels, it is worthwhile to observe global signal correlation (GSC) at the level of brain networks. Each scan's spatiotemporal matrix may be segmented into maximally independent components via independent component analysis (ICA) (McKeown et al., 1997). The brain networks segmented via ICA bear strong correspondence to brain networks identified via more direct indicators of coordinated neuronal activity, and they are, therefore, a useful tool in reorganizing voxel-wise BOLD signals into a reduced dataset that

*https://www.nitrc.org/projects/fcon_1000
†http://fcon_1000.projects.nitrc.org
‡www.fil.ion.ucl.ac.uk/spm/

better reflects the brain's internal organization (Smith et al., 2009). ICA analysis was performed by using the infomax algorithm in version 4.0a of the GIFT toolbox (Calhoun et al., 2001). A total of 18 components were estimated as optimal by using minimum-description-length criteria (Calhoun et al., 2001; Majeed and Avison, 2014). Components were stabilized by using six randomly initialized runs (Himberg et al., 2004). An additional six components were added to center the variability in components across runs, bringing the total number of independent components to 24.

The brain must also organize information across multiple time scales. Indeed, the power spectrum of the BOLD signal is inversely proportional to signal frequency, indicating the presence of long-memory processes (Billings et al., 2017; Bullmore et al., 2003; Chang and Glover, 2010; He, 2014; Wornell, 1993). Therefore, it is of interest to observe the GSC across multiple frequency bands, operating within a range of functional networks. To accomplish this, we spectrally segmented voxel-wise BOLD activations using Daubechies 7-tap wavelet in a discrete wavelet transform (Daubechies, 1988; Kronland-Martinet et al., 1987). Spectrally delimited global signals and independent components were generated by sampling from each volunteer's movement-corrected and filtered BOLD data. We further elaborate on the unstable nature of BOLD activations by calculating the instantaneous magnitude-squared coherence between the global bold signal and a set of independent components. This was accomplished by using an analytic Morlet wavelet distributed over a continuous range of scales (Maraun et al., 2007).

Results

Initial investigations into the spatial arrangement of BOLD GSC identified, on average, substantial positive zero-lag correlation with voxels throughout the brain (Fig. 1). GSC was particularly strong in the cortical gray matter and the dorsal CSF. GSC magnitude tended to decrease deep into the body, for example, in the orbito-frontal cortex and brain stem. Some reduction in the GSC was observed in the precuneus. Deep white matter regions approached mean zero GSC. The increase in GSC toward the peripheral white matter may owe itself to inaccuracies in group registration as well as from a generous white matter mask. Further investigation into the variation in GSC across individuals highlights regions in the dorsal aspect of the cranium with a large correlation standard deviation of ±0.3 (Fig. 2).

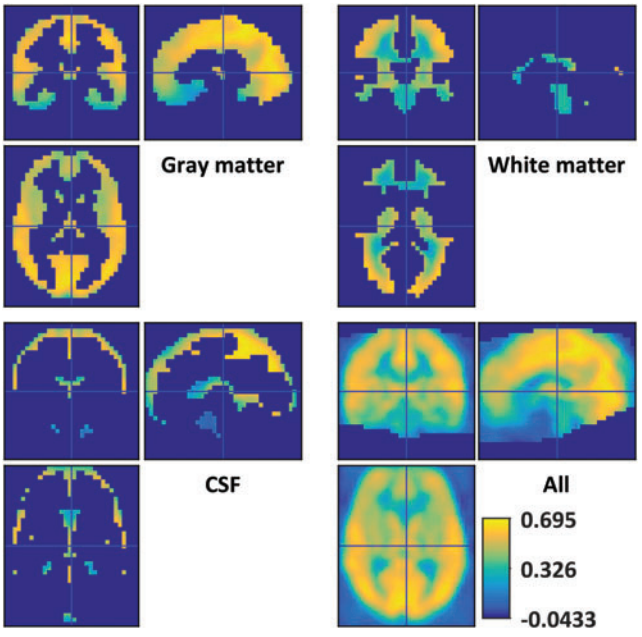

FIG. 1. Correlation between the global BOLD signal and voxel-wise signals separated by tissue type. Correlation is strongest in the gray matter but lacks cortical specificity. BOLD, blood oxygen level-dependent; CSF, cerebrospinal fluid. Color images available online at www.liebertpub.com/brain

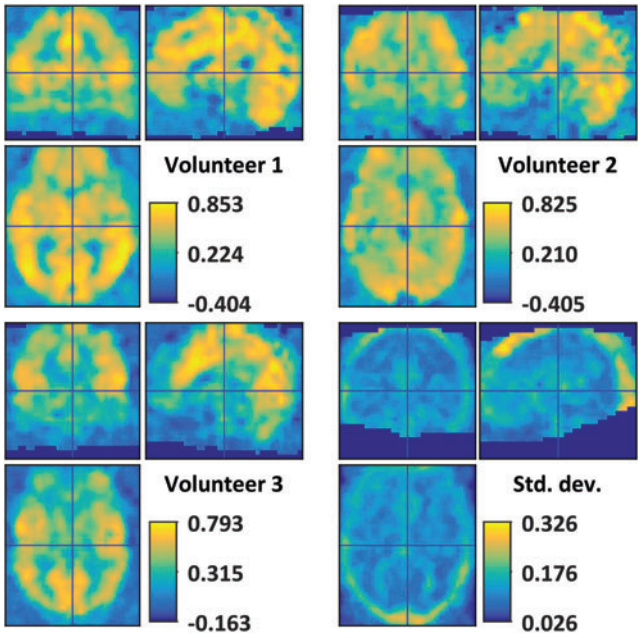

FIG. 2. Variation of GSC across volunteers. Registration mismatches likely contribute to strong GSC variation in extra-cerebral tissues. GSC, global signal correlation. Color images available online at www.liebertpub.com/brain

If GSC contributes to QPPs, we would expect to observe a spatiotemporal structure to GSC similar to that observed in QPPs; namely, fluctuations in the strength of correlation between the default mode and the task positive networks over the course of ~30 sec. The GSC is most strongly correlated with all voxel signals at time lag zero (Fig. 3A, B). Although it is possible to observe slight periodic correlations within the global signal itself, these were not specific to a brain region nor to a tissue class (Fig. 3A). Deviations from zero lag were only observed in ventral gray matter areas, that is, the cerebellum and in the orbitofrontal cortex (Fig. 3B). This observation may owe itself to a combination of registration inaccuracies, eye motion, and susceptibility mismatches between the gray matter and the eyes. The QPPs have some rhythmicity around the period of ~20 to 30 sec. If the global signal were to contribute to QPPs, there may be a peak in the QPP power spectrum around 0.25 to 0.17 Hz. Taking the power spectrum via Welch's method, the global signal did not present clear periodicities in the QPP's preferred frequency range (Fig. 3C).

If the global signal is not correlated with QPP activity, it may bear differential correlation with the activity of individual

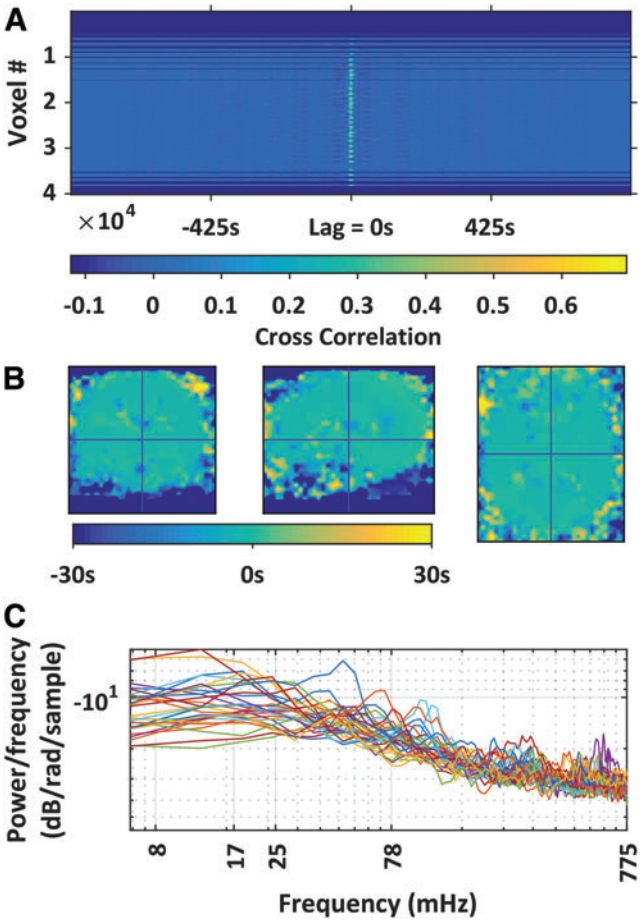

FIG. 3. **(A)** Observes the cross-correlation between the global BOLD signal (global signal) and all voxels. The time lag for maximum correlation was centered around 0 lag for most voxels. Although some faint periodicity exists, it is not specific to any tissue class or set of voxels. **(B)** Observes the lag for maximum correlation between the global BOLD signal and each voxel. Lag range is limited to ±30 sec to highlight possible relationships to quasi-periodic patterns observed to have a period of ~30 sec (Majeed et al., 2009). **(C)** Observes the frequency spectrum of the global signal from each volunteer. Color images available online at www.liebertpub.com/brain

brain networks. Figure 4 displays group mean GSC as a function of brain network and signal spectrum (Corresponding spatial ICA component maps may be found in the Supplementary Data; Supplementary Data are available online at www.liebertpub.com/brain). Networks were organized in terms of their relative functional connectivity (i.e., Pearson correlation) (Fig. 4C). Components related to physiological noise—eye motion (#'s 4, 9, and 14), head motion (#1)—tended to segment on the right side of the figure, and they were uncorrelated with the global signal (Fig. 4A). By contrast, a range of functional connectivity networks were highly correlated with the global signal. These networks included the basal ganglia (#8), the dorsal visual stream (#11), the DMN (#12), and the frontal cortex (#22). GSC among these networks tended to be in the low-frequency fluctuation range, ~10–200 mHz. Signals originating in the veins (#10) also showed strong GSC, although at lower frequencies than gray matter components. The strongest GSC variability across volunteers occurred in the lowest frequencies (2–6 mHz), where short scan lengths limit the number of low-frequency observations (Fig. 4B).

Although GSC variance across volunteers tended to be lowest where mean GSC magnitude was the highest (Fig. 4A, B), the time-varying nature of the BOLD signal warrants further detailing of intra-network GSC. Figure 5 provides a limited window on GSC temporal variability by plotting instantaneous GSC coherence with two contrasting functional networks from three volunteers: component #11 in the visual network (Fig. 5A) and component #12 in the DMN (Fig. 5B). In all cases, GSC is not a static quantity, but it fluctuates in magnitude over time. Of note is an absence of a consistent spatiotemporal structure.

Discussion

Spatial distribution of global signal

In agreement with previous research (Fox et al., 2009), the GSC was found to be the strongest in cortical gray matter. Within the gray matter, GSC appears to prefer some functional networks over others. Indeed, the primary visual cortex (component #3) demonstrated reduced GSC compared with its dorsal stream (#11). The same may be said for the strong activation in the DMN (#12) relative to its more ventro-lateral aspect (#18). Strong GSC outside gray matter tended to be confined to dorsal regions of the CSF, and could arise from a combination of greater coil sensitivity in those locations, as well as from partial volume effects at the CSF/gray matter tissue boundary. The same may be said for GSC in the white matter, where loss of signals and a generous white matter mask likely induce strong GSC in this tissue's periphery. These findings support a potential global but neural source as one contributor to the global BOLD signal.

Inter-individual differences. Registration mismatches and anatomical differences should account for some of the inter-individual variability, whereas nonstationarity in instantaneous global signal coherence supports the notion that inter-individual GSC variability may be partially explained by the individual's psycho-physical state. Indeed, the total DMN coherence appears less in volunteer 2 than in volunteers 1 and 3 (Fig. 5B). Inter-individual GSC variability warrants further examination as previous studies have demonstrated a relationship between inter-subject global signal variability and clinical pathology (Hahamy et al., 2014; Yang et al., 2014).

Role of QPPs in the global signal

We did not observe evidence of large-scale patterns or QPPs in the global signal (Amemiya et al., 2016; Majeed et al., 2011). We expected that strong contributions from these patterns would result in (1) dominance of the DMN or TPN as contributors to the global signal and/or (2) a spatially structured distribution of lag times that mapped to the known propagation of the patterns. Because neither of these was observed, we conclude that QPPs are not major contributors to the global signal and that GSR should not reduce sensitivity to the patterns.

These results may be predicted from the differences involved in the calculation of each quantity. QPPs represent average templates of discontinuous spatiotemporal BOLD

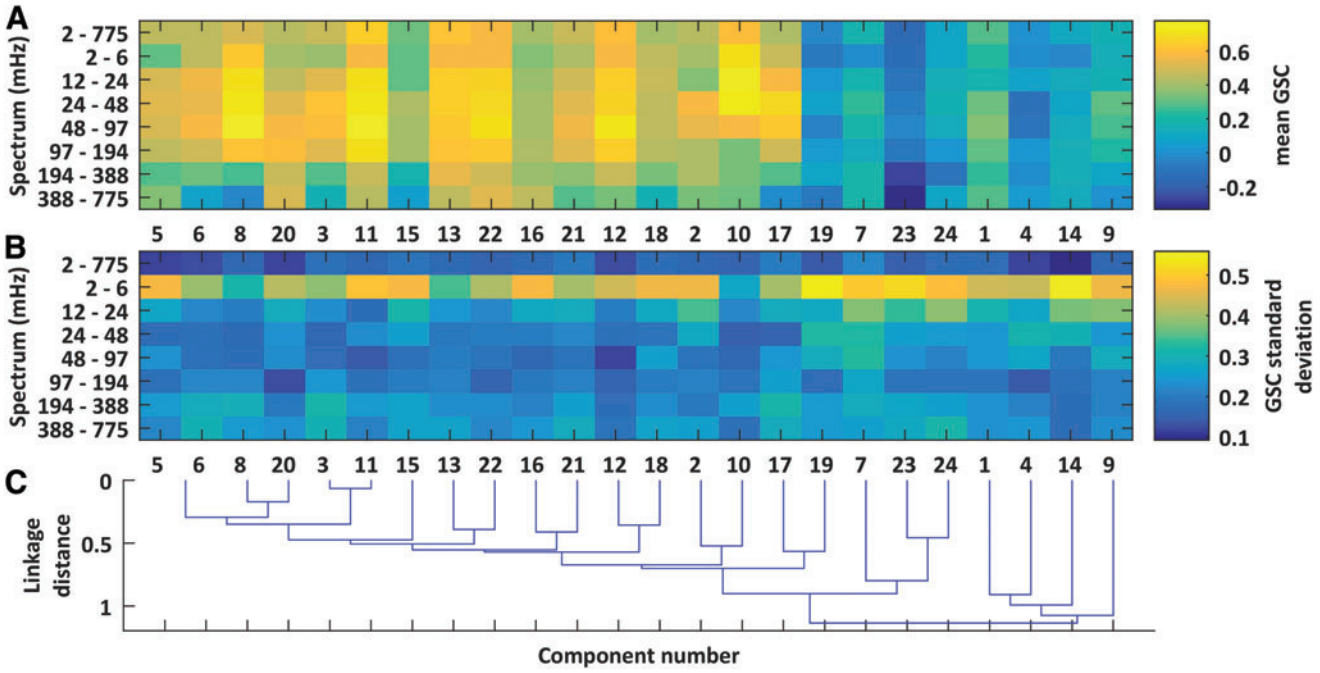

FIG. 4. The mean **(A)** and standard deviation **(B)** of global signal correlations after segmenting volunteer scans into multiple spatial and spectral components. Independent components were calculated across only gray matter voxels (upper two thirds of the gray-matters tissue probability map). The global signal included all voxels and also underwent spectral filtering. The dendrogram in **(C)** hierarchically orders components based on the average functional connectivity (Pearson correlation) between component time series. Color images available online at www.liebertpub.com/brain

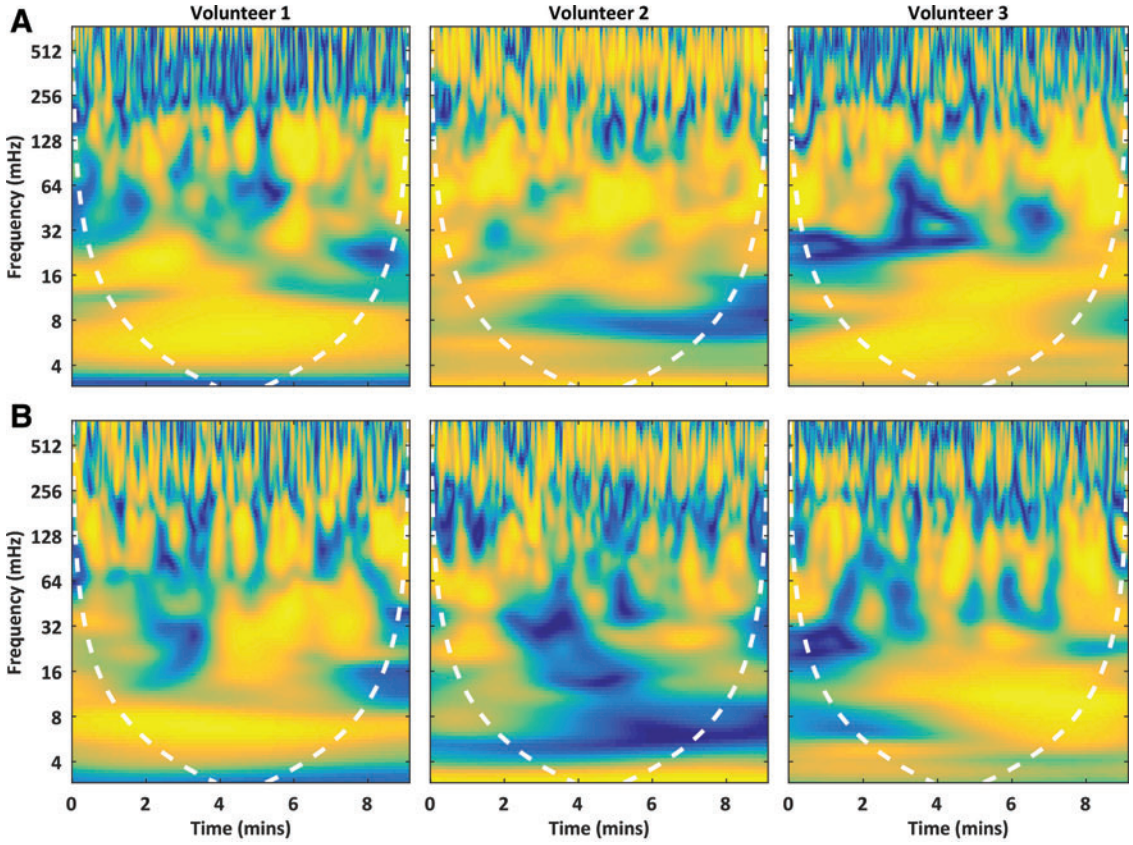

FIG. 5. Instantaneous magnitude-squared coherence between the global signal and either of two contrasting brain networks: the dorsal visual stream **(A)** (independent component #11) or the default mode network **(B)** (#12). The dashed line is a cone of influence demarcating the effective temporal limits of the spectral decomposition. Color images available online at www.liebertpub.com/brain

patterns, whereas the global signal is the instantaneous weighted sum of BOLD activations measured in a single individual's dynamically time-varying brain. After regressing the global signal from (z-scored) BOLD data, the resultant signal may be interpreted as a measure of each voxel's relative deviation from the global mean. GSR should, therefore, affect the observation of QPPs to the same extent that the QPP accounts for the total observed BOLD signal variance. However, the sliding correlation of the QPP template with the BOLD signal peaks at only ~ 0.4 (Yousefi et al., 2018). When QPP template correlation is low, other neuronal processes are contributing to the global signal.

GSR is, thus, qualitatively different from regression of a QPP template. This is in line with our previous finding that infraslow electrical activity was correlated to the BOLD signal regardless of whether GSR was applied (Pan et al., 2013). The lack of a spatially structured time lag is also in accordance with findings from a concurrent near-infrared spectroscopy and MRI study that found that hemodynamic lags varied by a second or less across the brain (Erdoğan et al., 2016). Further, our results are complementary to a recent publication by Yousefi et al. that showed that GSR changes the level of activity in the QPP, but not the spatial pattern or timing (Yousefi et al., 2018).

Vascular contributions

What is left in the global signal after motion parameter regression? One possibility is a vascular component. Indeed, component #10 includes the cranial veins and demonstrates strong GSC at lower frequencies. This result compares favorably with work by Tong and de Frederick showing that a peripheral measurement of hemodynamics is correlated with the BOLD signal over large swaths of the brain at different time lags (Tong and Frederick, 2010, 2014). These fluctuations could conceivably contribute to the global BOLD signal. Other vascular processes could also contribute. Vasomotion involves vascular oscillations at frequencies of ~ 0.1 Hz and remains poorly understood (Mayhew et al., 1996; Osol, 1988). Mayer waves, related to sympathetic nervous system oscillations, are another potential source of global signal oscillations (Julien, 2006). Future studies with other hemodynamic contrasts (cerebral blood volume [CBV], cerebral blood flow [CBF]) may help to shed light on the relative contribution of the vasculature to the BOLD global signal.

Neurophysiological origins

Recent work supports a neurophysiological origin for at least some portion of the global signal. A PET and rs-fMRI study in humans showed that the global signal amplitude was linked to changes in baseline FDG metabolism, whereas regional variance remained relatively unchanged by baseline metabolism (Thompson et al., 2016). In animal models, GSR has been used to control for different levels of baseline blood flow and metabolism in the brain due to varying levels of isoflurane anesthesia (Liu et al., 2013). Changes in broadband EEG power are associated with changes in global signal at delays approximating the hemodynamic delay (Wen and Liu, 2016). A number of EEG-MRI studies, particularly by Dr. Thomas Liu's group, have shown that the global signal amplitude is related to EEG measures of vigilance (Wong et al., 2013, 2016). Thus, the global signal may reflect large-scale modulation of brain activity related to fluctuations in arousal or vigilance levels. In a study that compared simultaneously recorded bandlimited power and BOLD correlation from two sites in the brain, GSR improved the fidelity of the BOLD signal to the changes in coordinated neural activity (Thompson et al., 2013b). This suggests that its removal may improve sensitivity to the coordinated, time-varying modulations of neural activity that would ideally be detected with rs-fMRI.

Conclusions

Though widespread, the global BOLD signal is not truly global, but rather tends to localize into a distributed set of gray matter networks and into regions spanned by the cranial veins. The strongest regional contributor to the global signal changes over the course of time and between individuals. However, this variability appears more chaotic than possessing large-scale quasi-periodic spatiotemporal organization. Inter-individual variations in the global signal motivate further examination to determine the variation's etiology and any diagnostic utility. Future work pursuing complementary measures of cerebral hemodynamics may help to disentangle these components.

Acknowledgments

This work was supported by NIH 5R01NS078095-02 and 3R01NS078095-02S1; and by Professional Development Supports Funds provided by Laney Graduate School, Emory University.

Author Disclosure Statement

No competing financial interests exist.

References

Abbas A, Majeed W, Thompson G, Keilholz SD. 2016. Phase of quasi-periodic patterns in the brain predicts performance on psychomotor vigilance task in humans. In Proceedings of the 24th Annual Meeting of ISMRM, Singapore, 2016, p. 1192.

Amemiya S, Takao H, Hanaoka S, Ohtomo K. 2016. Global and structured waves of rs-fMRI signal identified as putative propagation of spontaneous neural activity. Neuroimage 133:331–340.

Billings J, Medda A, Shakil S, Shen X, Kashyap A, Chen S, et al. 2017. Instantaneous brain dynamics mapped to a continuous state space. Neuroimage 162:344–352.

Biswal B, Yetkin FZ, Haughton VM, Hyde JS. 1995. Functional connectivity in the motor cortex of resting human brain using echo-planar MRI. Magn Reson Med 34:537–541.

Bullmore E, Fadili J, Breakspear M, Salvador R, Suckling J, Brammer M. 2003. Wavelets and statistical analysis of functional magnetic resonance images of the human brain. Stat Methods Med Res 12:375–399.

Buzsáki G, Draguhn A. 2004. Neuronal oscillations in cortical networks. Science 304:1926–1929.

Calhoun VD, Adali T, Pearlson GD, Pekar JJ. 2001. A method for making group inferences from functional MRI data using independent component analysis. Hum Brain Mapp 14:140–151.

Chang C, Glover GH. 2010. Time-frequency dynamics of resting-state brain connectivity measured with fMRI. Neuroimage 50: 81–98.

Daubechies I. 1988. Orthonormal bases of compactly supported wavelets. Commun Pure Appl Math 41:909–996.

Erdoğan SB, Tong Y, Hocke LM, Lindsey KP, deB Frederick B. 2016. Correcting for blood arrival time in global mean regression enhances functional connectivity analysis of resting state fMRI-BOLD signals. Front Hum Neurosci 10:311.

Fox MD, Snyder AZ, Vincent JL, Raichle ME. 2007. Intrinsic fluctuations within cortical systems account for intertrial variability in human behavior. Neuron 56:171–184.

Fox MD, Zhang D, Snyder AZ, Raichle ME. 2009. The global signal and observed anticorrelated resting state brain networks. J Neurophysiol 101:3270–3283.

Gonzalez-Castillo J, Saad ZS, Handwerker DA, Inati SJ, Brenowitz N, Bandettini PA. 2012. Whole-brain, time-locked activation with simple tasks revealed using massive averaging and model-free analysis. Proc Natl Acad Sci U S A 109: 5487–5492.

Hahamy A, Calhoun V, Pearlson G, Harel M, Stern N, Attar F, et al. 2014. Save the global: global signal connectivity as a tool for studying clinical populations with functional magnetic resonance imaging. Brain Connect 4:395–403.

He BJ. 2014. Scale-free brain activity: past, present, and future. Trends Cogn Sci 18:480–487.

Himberg J, Hyvarinen A, Esposito F. 2004. Validating the independent components of neuroimaging time series via clustering and visualization. Neuroimage 22:1214–1222.

Julien C. 2006. The enigma of Mayer waves: facts and models. Cardiovasc Res 70:12–21.

Kelly AM, Uddin LQ, Biswal BB, Castellanos FX, Milham MP. 2008. Competition between functional brain networks mediates behavioral variability. Neuroimage 39:527–537.

Kronland-Martinet R, Morlet J, Grossmann A. 1987. Analysis of sound patterns through wavelet transforms. Int J Pattern Recogn 1:273–302.

Liu X, Zhu X-H, Zhang Y, Chen W. 2013. The change of functional connectivity specificity in rats under various anesthesia levels and its neural origin. Brain Topogr 26:1–15.

Majeed W, Avison MJ. 2014. Robust data driven model order estimation for independent component analysis of fMRI data with low contrast to noise. PLoS One 9:e94943.

Majeed W, Magnuson M, Hasenkamp W, Schwarb H, Schumacher EHH, Barsalou L, Keilholz SDD. 2011. Spatiotemporal dynamics of low frequency BOLD fluctuations in rats and humans. Neuroimage 54:1140–1150.

Majeed W, Magnuson M, Keilholz SD. 2009. Spatiotemporal dynamics of low frequency fluctuations in BOLD fMRI of the Rat. J Magn Reson Imag 30:384–393.

Maraun D, Kurths J, Holschneider M. 2007. Nonstationary Gaussian processes in wavelet domain: synthesis, estimation, and significance testing. Phys Rev E 75:016707.

Mayhew JEW, Askew S, Zheng Y, Porrill J, Westby GWM, Redgrave P, et al. 1996. Cerebral vasomotion: a 0.1-Hz oscillation in reflected light imaging of neural activity. Neuroimage 4:183–193.

McKeown MJ, Makeig S, Brown GG, Jung T-P, Kindermann SS, Bell AJ, Sejnowski TJ. 1997. Analysis of fMRI data by blind separation into independent spatial components, Hum Brain Mapp 6:160–188.

Monto S, Palva S, Voipio J, Palva JM. 2008. Very slow EEG fluctuations predict the dynamics of stimulus detection and oscillation amplitudes in humans. J Neurosci 28: 8268–8272.

Murphy K, Birn RM, Bandettini PA. 2013. Resting-state fMRI confounds and cleanup. Neuroimage 80:349–359.

Murphy K, Birn RM, Handwerker DA, Jones TB, Bandettini PA. 2009. The impact of global signal regression on resting state correlations: are anti-correlated networks introduced? Neuroimage 44:893–905.

Nooner KB, Colcombe SJ, Tobe RH, Mennes M, Benedict MM, Moreno AL, et al. 2012. The NKI-Rockland sample: a model for accelerating the pace of discovery science in psychiatry. Front Neurosci 6:152. doi:10.3389/fnins.2012.00152

Osol G, Halpern W. 1988. Spontaneous vasomotion in pressurized cerebral arteries from genetically hypertensive rats. Am J Physiol 254:H28–H33.

Pan W-JJ, Thompson GJ, Magnuson ME, Jaeger D, Keilholz S. 2013. Infraslow LFP correlates to resting-state fMRI BOLD signals. Neuroimage 74:288–297.

Saad ZS, Gotts SJ, Murphy K, Chen G, Jo HJ, Martin A, Cox RW. 2012. Trouble at rest: how correlation patterns and group differences become distorted after global signal regression. Brain Connect 2:25–32.

Scholvinck ML, Maier A, Ye FQ, Duyn JH, Leopold DA. 2010. Neural basis of global resting-state fMRI activity. Proc Natl Acad Sci U S A 107:10238–10243.

Shirer WR, Jiang H, Price CM, Ng B, Greicius MD. 2015. Optimization of rs-fMRI pre-processing for enhanced signal-noise separation, test-retest reliability, and group discrimination. Neuroimage 117:67–79.

Smith SM, Fox PT, Miller KL, Glahn DC, Fox PM, Mackay CE, et al. 2009. Correspondence of the brain's functional architecture during activation and rest. Proc Nat Acad Sci U S A 106:13040–13045.

Thompson GJ, Magnuson ME, Merritt MD, Schwarb H, Pan WJ, Mckinley A, et al. 2013a. Short-time windows of correlation between large-scale functional brain networks predict vigilance intraindividually and interindividually. Hum Brain Mapp 34:3280–3298.

Thompson GJ, Merritt MD, Pan WJ, Magnuson ME, Grooms JK, Jaeger D, Keilholz SD. 2013b. Neural correlates of time-varying functional connectivity in the rat. Neuroimage 83:826–836.

Thompson GJ, Pan W-J, Billings JCW, Grooms JKK, Shakil S, Jaeger D, Keilholz SD. 2014a. Phase-amplitude coupling and infraslow (<1 Hz) frequencies in the rat brain: relationship to resting state fMRI. Front Integr Neurosci 8:41.

Thompson GJ, Pan W-J, Keilholz SD. 2015. Different dynamic resting state fMRI patterns are linked to different frequencies of neural activity. J Neurophysiol 114:114–124.

Thompson GJ, Pan WJ, Magnuson ME, Jaeger D, Keilholz SD. 2014b. Quasi-periodic patterns (QPP): large-scale dynamics in resting state fMRI that correlate with local infraslow electrical activity. Neuroimage 84:018–1031.

Thompson GJ, Riedl V, Grimmer T, Drzezga A, Herman P, Hyder F. 2016. The whole-brain ''global'' signal from resting state fMRI as a potential biomarker of quantitative state changes in glucose metabolism. Brain Connect 6:435–447.

Tong Y, Frederick BD. 2010. Time lag dependent multimodal processing of concurrent fMRI and near-infrared spectroscopy (NIRS) data suggests a global circulatory origin for

low-frequency oscillation signals in human brain. Neuroimage 53:553–564.

Tong Y, Frederick, BD. 2014. Tracking cerebral blood flow in BOLD fMRI using recursively generated regressors. Hum Brain Mapp 35:5471–5485.

Wen H, Liu Z. 2016. Broadband electrophysiological dynamics contribute to global resting-state fMRI signal. J Neurosci 36: 6030–6040.

Wong CW, DeYoung PN, Liu TT. 2016. Differences in the resting-state fMRI global signal amplitude between the eyes open and eyes closed states are related to changes in EEG vigilance. Neuroimage 124:24–31.

Wong CW, Olafsson V, Tal O, Liu TT. 2013. The amplitude of the resting-state fMRI global signal is related to EEG vigilance measures. Neuroimage 83:983–990.

Wornell GW. 1993. Wavelet-based representations for the 1/f family of fractal processes Proc IEEE 81:1428–1450.

Yang GJ, Murray JD, Repovs G, Cole MW, Savic A, Glasser MF, et al. 2014. Altered global brain signal in schizophrenia. Proc Natl Acad Sci U S A 111:7438–7443.

Yousefi B, Shin J, Schumacher EH, Keilholz SD. 2018. Quasi-periodic patterns of intrinsic brain activity in individuals and their relationship to global signal. Neuroimage 167: 297–308.

Address correspondence to:
Shella Keilholz
Department of Biomedical Engineering
Emory/Georgia Institute of Technology
1760 Haygood Drive
HSRB - W 230
Atlanta, GA 30322-4600

E-mail: shella.keilholz@bme.gatech.edu